Group 5 Metallocene Complexes as Models for Metal-Mediated Hydroboration: Synthesis of a Reactive Borane Adduct, *endo*-Cp*$_2$Nb($H_2BO_2C_6H_4$), via Hydroboration of Coordinated Olefins

Dean R. Lantero, Donald L. Ward,† and Milton R. Smith, III*

Contribution from the Department of Chemistry, Michigan State University, East Lansing, Michigan 48824

Received February 27, 1997[⊗]

Abstract: The olefin complexes Cp*$_2$M(CH_2═CH(R))(H) (R = H (**1**), CH_3 (**2**); M = Nb (**a**), Ta (**b**)) react cleanly with catecholborane (HBCat) and $HBO_2C_6H_3$-4-^{t}Bu (HBCat′) to give Cp*$_2$M(H_2BCat) (M = Nb (**5a**), Ta (**5b**)) and Cp*$_2$M(H_2BCat′) (M = Nb (**6a**), Ta (**6b**)) and the anti-Markovnikov hydroboration products CatBCH_2CH_2R and Cat′BCH_2CH_2R. Compounds **2a** and **2b** react with DBCat′ ($DBO_2C_6H_3$-4-^{t}Bu) to afford the deuterated analogs Cp*$_2$M(D_2BCat′) (M = Nb (**6a**), Ta (**6b**)) where the deuterium label is incorporated exclusively in the metal complex. The hydride resonances in **6a** exhibit large perturbations in chemical shift when deuterium is incorporated. On the basis of this isotopic labeling experiment, a mechanism is proposed where HBCat reacts with the 16-electron alkyl intermediates, Cp*$_2$MCH_2CH_2R (R = H (**3**), Me (**4**)), via σ-bond metathesis or oxidative-addition/reductive-elimination sequences, to generate the alkylboranes and an intermediate hydride, Cp*$_2$MH, that is trapped by additional borane to give Cp*$_2$M(H_2BCat) (**5a** and **5b**). The solid-state structures for Cp*$_2$Nb(η^2-$H_2BO_2C_6H_3$-3-^{t}Bu) (**16**) and Cp_2*Nb-(η^2-BH_4) (**17**) were determined by X-ray diffraction. The metal−boron distances in these two compounds are identical within experimental error. While related group 5 catecholateboryl compounds have pronounced boryl character, the structural parameters for the hydride and boryl ligands in **16** are consistent with formulation as either a borohydride complex or a borane adduct of "Cp*$_2$NbH". In contrast to other group 5 boryl complexes, **6a** reacts readily with various two-electron ligands with elimination of HBCat′. For example, H_2 reacts reversibly to form Cp*$_2$NbH_3 and HBCat′, while "BH_3" and CO react irreversibly to yield Cp*Nb(BH_4) and Cp*$_2$Nb(H)(CO) with elimination of HBCat′, respectively. Ethylene and propylene react at 40 °C to regenerate **1a** and **2a**, with elimination of HBCat′. When excess olefin is present, the liberated borane is converted to CatBCH_2CH_2R. Solutions of **1a** and **2a** catalyze olefin hydroboration under mild conditions. Relationships between the reactivity of **1a** and **2a** and other early metal and lanthanide catalysts are discussed.

Introduction

The hydroboration reaction is one of the most versatile methods for reduction of unsaturated carbon bonds. In contrast to hydrogenation, hydroboration yields products where the inherent functionality of the parent olefin is preserved and the resulting boron-carbon bond can serve as a synthon for various functional groups.[1] Importantly, these transformations generally proceed with retention of stereochemistry at carbon. This feature has sparked interest in controlling selectivity of B−H additions to olefins and alkynes. In this regard, metal−mediated hydroborations are attractive since selectivities dictated by a metal center may differ from those in uncatalyzed reactions.[2] Also, catalyzed additions by chiral complexes potentially offer enantioselectivity in the hydroboration of prochiral substrates.[3]

Most of the initial efforts in metal-mediated hydroboration focused on catalysis by late transition metals.[4,5] The mechanism(s) that operate in these systems have been the subject of several experimental and theoretical studies. Pathways involving oxidative addition/reductive elimination sequences were initially proposed based in part on precedent from hydrogenations by Wilkinson's catalyst[6] and the fact that oxidative addition of catecholborane to $(PPh_3)_3$RhCl gives $(PPh_3)_3$RhClHBCat.[7] Thorough examinations indicate that the reaction manifold is more complex.[5g−h,l] In attempts to resolve mechanistic issues,

† Author to whom crystallographic issues should be addressed.

⊗ Abstract published in *Advance ACS Abstracts,* August 15, 1997.

(1) Pelter, A.; Smart, K.; Brown, H. C. *Borane Reagents*; Academic Press: London, 1988; p 131.

(2) For a review of transition metal catalyzed hydroboration see: Burgess, K.; Ohlmeyer, M. J. *Chem. Rev.* **1991**, *91*, 1179−1191.

(3) Late transition-metal catalysts have been effective for asymmetric hydroborations of olefins: (a) Burgess, K.; Ohlmeyer, M. J. *J. Org. Chem.* **1988**, *53*, 5178−5179. (b) Hayashi, T.; Matsumoto, Y.; Ito, Y. *J. Am. Chem. Soc.* **1989**, *111*, 3426−3428. (c) Brown, J. M.; Hulmes, D. I.; Layzell, T. P. *J. Chem. Soc., Chem. Commun.* **1993**, 1673−1674.

(4) For metal-catalyzed additions of carboranes to olefins see: (a) Davan, T.; Corcoran, E. W.; Sneddon, L. G. *Organometallics* **1983**, *2*, 1693−1694. (b) Hewes, J. D.; Kreimendahl, C. W.; Marder, T. B.; Hawthorne, M. F. *J. Am. Chem. Soc.* **1984**, *106*, 5757−5759. (c) Mirabelli, M. G. L.; Sneddon, L. G. *J. Am. Chem. Soc.* **1988**, *110*, 449−453.

(5) For metal-catalyzed additions of catecholborane to olefins see: (a) Manning, D.; Nöth, H. *Angew. Chem., Int. Ed. Engl.* **1985**, *24*, 878−879. (b) Evans, D. A.; Fu, G. C.; Hoveyda, A. H. *J. Am. Chem. Soc.* **1988**, *110*, 6917−6918. (c) Burgess, K.; Ohlmeyer, M. J. *Tetrahedron Lett.* **1989**, *30*, 395−398, 5857−5860, 5861−5864. (d) Burgess, K.; van der Donk, W. A.; Jarstfer, M. B.; Ohlmeyer, M. J. *J. Am. Chem. Soc.* **1991**, *113*, 6139−6144. (e) Burgess, K.; Cassidy, J.; Ohlmeyer, M. J. *J. Org. Chem.* **1991**, *56*, 1020−1027. (f) Evans, D. A.; Fu, G. C.; Hoveyda, A. H. *J. Am. Chem. Soc.* **1992**, *114*, 6671−6679. (g) Evans, D. A.; Fu, G. C.; Anderson, B. A. *J. Am. Chem. Soc.* **1992**, *114*, 6679−6685. (h) Westcott, S. A.; Blom, H. P.; Marder, T. B.; Baker, R. T. *J. Am. Chem. Soc.* **1992**, *114*, 8863−8869. (i) Burgess, K.; van der Donk, W. A.; Westcott, S. A.; Marder, T. B.; Baker, R. T.; Calabrese, J. C. *J. Am. Chem. Soc.* **1992**, *114*, 9350−9359. (j) Westcott, S. A.; Marder, T. B.; Baker, R. T. *Organometallics* **1993**, *12*, 975−979. (k) Westcott, S. A.; Blom, H. P.; Marder, T. B.; Baker, R. T.; Calabrese, J. C. *Inorg. Chem.* **1993**, *32*, 2175−2182.

(6) Collman, J. P.; Hegedus, L. S.; Norton, J. R.; Finke, R. G. *Principles and Applications of Organotransition Metal Chemistry*; University Science Books: Mill Valley, 1987; Chapter 10.

(7) Kono, H.; Ito, K.; Nagai, Y. *Chem. Lett.* **1975**, 1095−1096.

S0002-7863(97)00639-2 CCC: $14.00

potential pathways have been evaluated by computational methods. Mechanisms involving oxidative addition/reductive elimination sequences seem to be preferred; however, a clear consensus has not been reached and mechanisms where σ-bond metatheses operate in lieu of oxidative addition/reductive elimination are not prohibitively disfavored.[8] While labeling experiments are consistent with oxidative addition/reductive elimination mechanisms,[5g] mechanisms involving σ-bond metatheses cannot be categorically excluded given precedent in late metal systems.[9]

By comparison, forays in early transition-metal and lanthanide systems have been fewer.[10,11] When catecholborane (HBCat) is employed as the borane reagent, complications can arise from incompatibility between the catalyst and borane reagent, particularly when the metal−center and borane are supported by labile alkoxide ligands.[11b,c] These problems are not necessarily general as recent reports indicate that group 4 metallocene complexes catalyze addition of HBCat to olefins where key hydroboration steps likely occur at the metal−center.[11a,12] Metallocene systems are attractive as cyclopentadienyl ligands and are relatively inert, and thus provide a well-defined coordination sphere for the metal.

We have been examining the reactivity of B−H bonds with metallocene olefin complexes.[12] Apart from the reasons outlined above, the chemistry of these species with borane reagents offers interesting possibilities since the metal−carbon bonds exhibit reactivity that is consistent with pronounced metallacyclopropane character in the metal−olefin moiety. Thus, ring-opening σ-bond metathesis between B−H and M−C bonds offers a pathway for B−C bond formation that is mechanistically distinct from those postulated in late-metal and lanthanide systems. Borylation by these routes can lead to unusual selectivities, as illustrated by the fact that $Cp^*_2Ti(\eta^2\text{-}CH_2{=}CH_2)$ reacts with catecholborane, and related borane reagents, via a dehydrogenative pathway where borylation proceeds without bond reduction.

This reactivity prompted us to examine the chemistry of the olefin−hydride complexes $Cp^*_2M(CH_2{=}CH(R))(H)$ (R = H (**1**), CH_3 (**2**); M = Nb (**a**), Ta (**b**)).[13] In these systems, insertion of the coordinated olefin into the metal−hydride bond to form alkyl intermediates is well-documented. Hence, investigating the reaction chemistry of **1** and **2** with borane reagents offers an interesting comparison between relative reactivities of the olefin−hydride resting states and the alkyl intermediates. Given well-behaved reactivity, we felt that these systems would be ideally suited for mechanistic investigations; this paper describes the results.

Experimental Section

General Considerations. All manipulations were performed using glovebox, Schlenk, and vacuum-line techniques. Pentane, heptane, THF, and toluene were predried over sodium. Toluene was distilled from NaK/benzophenone ketyl. All other solvents were distilled from sodium/benzophenone ketyl. Benzene-d_6 and toluene-d_8 were dried over activated 3 Å molecular sieves and then vacuum transferred into a sodium mirrored container. Argon and nitrogen gases were purified by passage over MnO on silica.

Catecholborane (Aldrich) was vacuum transferred prior to use. Preparation of the other boranes was accomplished by reacting $NaBH_4$ (or $NaBD_4$) (Aldrich) and $BF_3{\cdot}OEt_2$ (Mallinckrodt) to produce BH_3 (or BD_3), which was then bubbled through THF solutions of the appropriate diol (4-*tert*-butylcatechol (Aldrich) or 3-*tert*-butylcatechol).[14] The THF was then distilled from the solution at atmospheric pressure, and the remaining solution was vacuum distilled to give the borane as a clear, viscous liquid. Styrene and 1-hexene (Aldrich) were dried over activated 3 Å molecular sieves and vacuum transferred prior to use. Phenethyl alcohol and *sec*-phenethyl alcohol (both Aldrich) were used as received. *cis*-Cyclooctene (Aldrich) was distilled prior to use. Ethylene (Matheson) and propylene (Matheson) were subjected to several freeze−pump−thaw cycles and then transferred in vacuo to reaction vessels. Carbon monoxide (Matheson) and dihydrogen (AGA Gas Inc.) were used as received. $Cp^*_2NbH(C_3H_6)$,[13a] Cp_2NbBH_4,[15] $Cp^*_2TaH(C_3H_6)$,[16] and $Cp^*_2Nb(BH_4)$[17] were prepared by literature methods.

^{1}H NMR spectra were recorded on Varian Gemini-300 (300.0 MHz), Varian VXR-300 (299.9 MHz), and Varian VXR-500 (499.9 MHz) spectrometers and referenced to residual proton solvent signals. ^{2}H NMR spectra were recorded on a Varian VXR-300 spectrometer operating at 46.0 MHz, and spectra were referenced to residual deuterium signals of the proteo solvent. ^{11}B NMR spectra were recorded on a Varian VXR-300 spectrometer operating at 96.23 MHz and spectra were referenced to a $BF_3{\cdot}Et_2O$ external standard solution. Infrared spectra were recorded as Nujol mulls in KBr plates with a Nicolet IR/42 spectrometer. GC samples were run on a Hewlett Packard 5890A gas chromatograph equipped with a Hewlett Packard 3392 integrator and a Foxboro GB-1 capillary column (25 m × 0.25 mm i.d. with a 0.25 μm film). Elemental analyses were performed by Desert Analytics, Tucson, AZ.

Procedures: *endo*-$Cp^*_2Nb(H_2BO_2C_6H_4)$ (5a). A 15-mL toluene solution of $Cp^*_2NbH(C_3H_6)$ (219 mg, 0.540 mmol) was cooled to −78 °C. Catecholborane (0.161 mL, 1.35 mmol) was added to this stirred solution via syringe. The resulting mixture was warmed to room temperature and stirred for 2 h. During the course of the reaction, the color of the solution gradually lightened from deep red to orange-red, and solvent evaporation gave a deep orange solid. The reaction mixture was dissolved in a minimal volume of toluene and cooled to −80 °C. The product was isolated as orange microcrystals (207 mg, 79%): mp 171−3 °C; ^{1}H NMR (C_6D_6) δ 7.07 (m, 2H, $O_2C_6H_4$), 6.85 (m, 2H, $O_2C_6H_4$), 1.83 (s, 30H $C_5(CH_3)_5$), −8.27 (br, 2H, NbH_2); ^{11}B NMR (C_6D_6) δ 60.2 ($\Delta\nu_{1/2}$ = 240 Hz); IR (cm^{-1}) 1653 (ν_{NbH}). Anal. Calcd for $C_{26}H_{36}BNbO_2$: C, 64.5; H, 7.44. Found: C, 64.1; H, 7.26.

(8) For BH_3 additions mediated by 14-electron intermediates, computations favor B−H oxidative addition, olefin insertion into the Rh−H bond, followed by B−C reductive elimination of the alkylborane product.[8a] For $HB(OH)_2$ additions effected by 16-electron intermediates, computations favor B−H oxidative addition, olefin insertion into the Rh−B bond, and C−H reductive elimination to generate alkylboronate ester.[8b,c] In the latter study, the barrier for a pathway involving σ-bond metathesis was only 1.5 kcal/mol higher than the oxidative addition pathway. While addition of $HB(OH)_2$ is more relevant to catalyzed addition of HBCat, pathways involving 14-electron intermediates have not been considered.[8c] (a) Dorigo, A. E.; Schleyer, P. v. R. *Angew. Chem., Int. Ed. Engl.* **1995**, *34*, 115−118. (b) Musaev, D. G.; Mebal, A. M.; Morokuma, K. *J. Am. Chem. Soc.* **1994**, *116*, 10693−10792. (c) Musaev, D. G.; Matsubara, T.; Mebal, A. M.; Koga, N.; Morokuma, K. *Pure Appl. Chem.* **1995**, *67*, 257−263.

(9) (a) Hartwig, J. F.; Bhandari, S.; Rablen, P. R. *J. Am. Chem. Soc.* **1994**, *116*, 1839−1844. (b) Baker, R. T.; Calabrese, J. C.; Westcott, S. A.; Marder, T. B. *J. Am. Chem. Soc.* **1995**, *117*, 8777−8784.

(10) Harrison, K. M.; Marks., T. J. *J. Am. Chem. Soc.* **1992**, *114*, 9220−9221.

(11) (a) Erker, G.; Noe, R.; Wingbermühle, D.; Petersen, J. L. *Angew. Chem., Int. Ed. Engl.* **1993**, *32*, 1213−1215. (b) Burgess, K.; Jaspars, M. *Tetrahedron Lett.* **1993**, *34*, 6813−6816. (c) Burgess, K.; van der Donk, W. A. *Organometallics* **1994**, *13*, 3616−3620. (d) Bijpost, E. A.; Duchateau, R.; Teuben, J. H. *J. Mol. Catal. A: Chem.* **1995**, *95*, 121−128. (e) Pereira, S.; Srebnik, M. *Organometallics* **1995**, *14*, 3127−3128. (f) Pereira, S.; Srebnik, M. *J. Am. Chem. Soc.* **1996**, *118*, 909−910. (g) He, X.; Hartwig, J. F. *J. Am. Chem. Soc.* **1996**, *118*, 1696−1702.

(12) (a) Motry, D. H.; Smith, M. R., III *J. Am. Chem. Soc.* **1995**, *117*, 6615−6616. (b) Motry, D. H.; Brazil, A. G.; Smith, M. R., III *J. Am. Chem. Soc.* **1997**, *119*, 2743−2744.

(13) (a) Doherty, N. M.; Bercaw, J. E. *J. Am. Chem. Soc.* **1985**, *107*, 2670−2682. (b) Burger, B. J.; Santarsiero, B. D.; Trimmer, M. S.; Bercaw, J. E. *J. Am. Chem. Soc.* **1988**, *110*, 3134−3146.

(14) Hocking, M. B. *Can. J. Chem.* **1973**, *51*, 2384−2392.

(15) Lucas, C. R.; Green, M. L. H. *J. Chem. Soc., Chem. Commun.* **1972**, 1005.

(16) Gibson, V. C.; Bercaw, J. E.; Bruton, W. J.; Sanner, R. D. *Organometallics* **1986**, *5*, 976−979.

(17) Bell, R. A.; Cohen, S. A.; Doherty, N. M.; Threlkel, R. S.; Bercaw, J. E. *Organometallics* **1986**, *5*, 972−975.

(18) Brown, H. C.; Gupta, S. K. *J. Am. Chem. Soc.* **1975**, *97*, 5249−5255.

***endo*-Cp*$_2$Nb(H$_2$BO$_2$C$_6$H$_3$-4-^{t}Bu) (6a).** A 20-mL toluene solution of Cp*$_2$NbH(C$_3$H$_6$) (400 mg, 0.985 mmol) was cooled to −78 °C. HBO$_2$C$_6$H$_3$-4-^{t}Bu (0.360 mL, 2.07 mmol) was then added via syringe to the stirred solution, and the mixture was warmed to room temperature. After 2 h, the toluene was removed in vacuo, leaving a viscous red oil. The oil was dissolved in a minimal volume of heptane and placed in a −80 °C freezer. Upon standing overnight, deep red microcrystals were deposited. After the filtrate was removed, the crystals were washed with cold pentane and dried in vacuo (396 mg, 75%): mp 154−7 °C; ^{1}H NMR (C$_6$D$_6$) δ 7.30 (d, J = 2.1 Hz, 1H, O$_2$C$_6$*H$_3$*), 7.04 (d, J = 8.1 Hz, 1H, O$_2$C$_6$*H$_3$*), 6.90 (dd, J = 7.8, 1.95 Hz, 1H, O$_2$C$_6$*H$_3$*), 1.85 (s, 30H C$_5$(C*H$_3$*)$_5$), 1.30 (s, 9H O$_2$C$_6$H$_3$(4-C(C*H$_3$*)$_3$), −8.19 (br, 2H, Nb*H$_2$*); ^{11}B NMR (C$_6$D$_6$) δ 60.0 ($\Delta\nu_{1/2}$ = 300 Hz); IR (cm^{-1}) 1653 (ν_{NbH}). ***endo*-Cp*$_2$Nb(D$_2$BO$_2$C$_6$H$_3$-4-^{t}Bu)** was similarly prepared from Cp*$_2$NbH(C$_3$H$_6$) and DBO$_2$C$_6$H$_3$-4-^{t}Bu: ^{1}H NMR (C$_6$D$_6$) δ 7.28 (d, J = 1.8 Hz, 1H, O$_2$C$_6$*H$_3$*), δ 7.03 (d, J = 8.1 Hz, 1H, O$_2$C$_6$*H$_3$*), δ 6.89 (dd, J = 8.1, 1.95 Hz, 1H, O$_2$C$_6$*H$_3$*), δ 1.83 (s, 30H C$_5$(C*H$_3$*)$_5$), δ 1.30 (s, 9H O$_2$C$_6$H$_3$(4-C(C*H$_3$*)$_3$); ^{2}H NMR (C$_6$H$_6$) δ −9.29 (br, Nb*D$_2$*); ^{11}B NMR (C$_6$D$_6$) δ 57.3 ($\Delta\nu_{1/2}$ = 266 Hz).

***endo*-Cp*$_2$Nb(H$_2$BO$_2$C$_6$H$_3$-3-^{t}Bu) (16).** A 10-mL toluene solution of Cp*$_2$NbH(C$_3$H$_6$) (251 mg, 0.618 mmol) was cooled to −78 °C. HBO$_2$C$_6$H$_3$-3-^{t}Bu (229 mg, 1.30 mmol) was dissolved in ∼5 mL of toluene, and the borane solution was transferred to the propylene−hydride complex via cannula. Once the addition was complete, the resulting solution was allowed to warm to room temperature and stirred for 3 h. The toluene was then evaporated, leaving a tacky, deep orange-red solid. The crude mixture was dissolved in a minimal volume of pentane and placed in a −80 °C freezer. Orange-red microcrystals were deposited overnight. The product was collected, washed with cold pentane, and dried in vacuo (218 mg, 65%): mp 141−2 °C; ^{1}H NMR (C$_6$D$_6$) δ 7.04 (m, 1H, O$_2$C$_6$*H$_3$*), 6.96 (m, 1H, O$_2$C$_6$*H$_3$*), 6.91 (m, 1H, O$_2$C$_6$*H$_3$*), 1.86 (s, 30H C$_5$(C*H$_3$*)$_5$), 1.58 (s, 9H O$_2$C$_6$H$_3$(4-C(C*H$_3$*)$_3$), -7.91 (br, 2H, Nb*H$_2$*); ^{11}B NMR (C$_6$D$_6$) δ 60.9 ($\Delta\nu_{1/2}$ = 280 Hz); IR (cm^{-1}) 1649 (ν_{NbH}).

***endo*-Cp*$_2$TaH$_2$(BO$_2$C$_6$H$_4$) (5b).** Catecholborane (0.120 mL, 0.973 mmol) was added to a 10-mL toluene solution of Cp*$_2$TaH(C$_3$H$_6$) (193 mg, 0.389 mmol) at room temperature. The solution was then stirred for 2 h during which time the initial pale yellow color gradually turned a lime green. Evaporation of the toluene yielded a lime green solid. Washing this solid with pentane followed by drying under vacuum yielded a pale yellow solid (160 mg, 72%): mp 159−62 °C dec; ^{1}H NMR (C$_6$D$_6$) δ 7.19 (m, 2H, O$_2$C$_6$*H$_4$*), 6.89 (m, 2H, O$_2$C$_6$*H$_4$*), 1.96 (s, 30H C$_5$(C*H$_3$*)$_5$), −2.12 (br, 2H, Ta*H$_2$*); ^{11}B NMR (C$_6$D$_6$) δ 73.5 ($\Delta\nu_{1/2}$ = 390 Hz); IR (cm^{-1}) 1774, 1709 (ν_{TaH}).

***endo*-Cp*$_2$TaH$_2$(BO$_2$C$_6$H$_3$-4-^{t}Bu) (6b).** Toluene (∼5 mL) was used to dissolve Cp*$_2$TaH(C$_3$H$_6$) (155 mg, 0.313 mmol). HBO$_2$C$_6$H$_3$-4-^{t}Bu (0.140 mL, 0.784 mmol) was then added via syringe to the stirred solution. The resulting solution was stirred for 2 h at room temperature, giving a rust orange solution. Evaporation of the toluene yielded a viscous, deep orange oil. Dissolving this oil in pentane and concentrating the resulting orange solution yielded pale yellow microcrystals when placed in a −80 °C freezer overnight. Separating the filtrate and drying the microcrystals under vacuum gave the pure product (112 mg, 57%): mp 156−8 °C; ^{1}H NMR (C$_6$D$_6$) δ 7.42 (d, J = 2.1 Hz, 1H, O$_2$C$_6$*H$_3$*), δ 7.19 (d, J = 11.4 Hz, 1H, O$_2$C$_6$*H$_3$*), δ 6.95 (dd, J = 8.4, 1.95 Hz, 1H, O$_2$C$_6$*H$_3$*), δ 1.98 (s, 30H C$_5$(C*H$_3$*)$_5$), δ 1.29 (s, 9H O$_2$C$_6$H$_3$-(4-C(C*H$_3$*)$_3$), δ −2.05 (s, 2H, Ta*H$_2$*); ^{11}B NMR (C$_6$D$_6$) δ 72.7 ($\Delta\nu_{1/2}$ = 610 Hz); IR (cm^{-1}) 1767, 1720 (ν_{TaH}). Anal. Calcd for C$_{30}$H$_{44}$BO$_2$Ta: C, 57.4; H, 7.01. Found: C, 57.6; H, 7.29. ***endo*-Cp*$_2$TaD$_2$-(BO$_2$C$_6$H$_3$-4-^{t}Bu)** was similarly prepared from Cp*$_2$TaH(C$_3$H$_6$) and DBO$_2$C$_6$H$_3$-4-^{t}Bu: ^{1}H NMR (C$_6$D$_6$) δ 7.41 (d, J = 1.8 Hz, 1H, O$_2$C$_6$*H$_3$*), 7.18 (d, J = 8.1 Hz, 1H, O$_2$C$_6$*H$_3$*), 6.95 (dd, J = 8.1, 1.8 Hz, 1H, O$_2$C$_6$*H$_3$*), 1.97 (s, 30H, C$_5$(C*H$_3$*)$_5$), 1.29 (s, 9H, O$_2$C$_6$H$_3$(4-C(C*H$_3$*)$_3$)); ^{2}H NMR (C$_6$H$_6$) δ −2.02 (br, Ta*D$_2$*); ^{11}B NMR (C$_6$D$_6$) δ 72.3 ($\Delta\nu_{1/2}$ = 660 Hz). **6b**-d_{0-2} was prepared as a mixture of isotopomers by adding equal volumes of HBO$_2$C$_6$H$_3$-4-^{t}Bu and DBO$_2$C$_6$H$_3$-4-^{t}Bu to a toluene solution of Cp*$_2$TaH(C$_3$H$_6$). The workup was analogous to that described above: ^{1}H NMR (C$_6$D$_6$) δ 7.41 (m 1H, O$_2$C$_6$*H$_3$*), 7.17 (m, 1H, O$_2$C$_6$*H$_3$*), 6.82 (m, 1H, O$_2$C$_6$*H$_3$*), 1.98 (s, 30H C$_5$(C*H$_3$*)$_5$), 1.29 (s, 9H O$_2$C$_6$H$_3$(4-C(C*H$_3$*)$_3$)), −2.06 (s, 1H, Ta*H*D); ^{2}H NMR (C$_6$H$_6$) δ −2.02 (br, TaH*D*); ^{11}B NMR (C$_6$D$_6$) δ 70.0 ($\Delta\nu_{1/2}$ = 650 Hz).

Phenethyl Alcohol Formation. Cp*$_2$NbH(C$_3$H$_6$) (15.3 mg, 0.038 mmol) was dissolved in ∼0.6 mL of benzene-d_6 along with styrene (63.1 mg, 0.607 mmol) and HBO$_2$C$_6$H$_3$-4-^{t}Bu (106 mg, 0.602 mmol). The solution was placed in an NMR tube and flame sealed. The tube was then maintained at 75 °C for 4 days in a constant temperature oil bath. Conversion of free borane to the alkyl borane product was monitored by ^{1}H NMR. Integration revealed 64% hydroborated products along with 11% of a boron decomposition product[5k,11b] and 25% unreacted borane. The contents were then converted to the corresponding alcohol by a literature method.[18] The products of the oxidative workup were analyzed by gas chromatography, with phenethyl alcohol and *sec*-phenethyl alcohol detected in a 3.72:1 ratio.

NMR Tube Reactions: Cp*$_2$NbH(C$_3$H$_6$) + *cis*-cyclooctene + HBO$_2$C$_6$H$_3$-4-^{t}Bu. Cp*$_2$NbH(C$_3$H$_6$) (11.8 mg, 0.029 mmol) was dissolved in ∼0.6 mL of benzene-d_6 along with *cis*-cyclooctene (3.2 mg, 0.029 mmol) and HBO$_2$C$_6$H$_3$-4-^{t}Bu (4.4 mg, 0.025 mmol). The resulting solution was transferred to a NMR tube that was flame sealed. The tube was kept at room temperature for 2.5 h. A ^{1}H NMR spectrum showed primary hydroboration occurred with the bound propylene fragment on the niobium complex with some hydroboration of the *cis*-cyclooctene. Integration of the appropriate ^{t}Bu resonances established the ratio of *cis*-cyclooctene:propylene hydroboration as 1:5.08. The tube was held at room temperature overnight, and integration of another ^{1}H NMR spectrum determined the ratio of *cis*-cyclooctene:propylene hydroboration to be 1:3.81.

Cp*$_2$NbH(C$_3$H$_6$) + *cis*-cyclooctene + propylene + HBO$_2$C$_6$H$_3$-4-^{t}Bu. Cp*$_2$NbH(C$_3$H$_6$) (9.8 mg, 0.024 mmol) was dissolved in ∼0.6 mL of benzene-d_6. HBO$_2$C$_6$H$_3$-4-^{t}Bu (51.0 mg, 0.290 mmol) and *cis*-cyclooctene (16.0 mg, 0.145 mmol) were added to the solution which was then placed in a NMR tube. The tube was then frozen with liquid nitrogen and evacuated. Propylene (0.145 mmol) was then admitted with the aid of a calibrated volume vessel. The NMR tube was then flame sealed, and the contents of the tube were heated at 60 °C for 3 days. The rate of hydroboration for propylene was faster than that of *cis*-cyclooctene based on integrated ^{1}H spectra (propylene:*cis*-cyclooctene = 4.53:1). Repeating the reaction without the use of the niobium complex required heating the reaction at 120 °C for 3 days and resulted in nearly identical rates of hydroboration; however, the rate for *cis*-cyclooctene was slightly faster (propylene:*cis*-cyclooctene = 0.93:1).

Cp*$_2$Nb(H$_2$BO$_2$C$_6$H$_4$) + CO. A 10-mg (0.021 mmol) sample was dissolved in ∼0.8 mL of benzene-d_6. This solution was placed in an NMR tube and frozen with liquid nitrogen. The NMR tube was then evacuated and 1 atm of CO gas admitted. The tube was then flame sealed and allowed to warm to room temperature. ^{1}H and ^{11}B NMR spectra indicated elimination of HBCat, and Cp*$_2$NbH(CO) was the only Nb-containing product detected. Integration of the ^{11}B spectrum indicated 91% catecholborane (δ 28.7, d, J_{HB} = 184 Hz) and 9% B$_2$Cat$_3$ (δ 22.7, s).

5a + B$_2$H$_6$. A 15-mg (0.031 mmol) sample of the niobium complex was dissolved in ∼0.6 mL of toluene-d_8 and placed in a NMR tube. The solution was frozen with liquid nitrogen and then evacuated. Diborane generation was performed in the following way: A Schlenk tube was charged with NaBH$_4$ (130 mg, 3.43 mmol) and DME (0.875 mL). This slurry was cooled in a liquid nitrogen bath, and BF$_3$·Et$_2$O (0.580 mL, 3.52 mmol) was added under a counter flow of N$_2$ gas. The Schlenk tube was fitted with an adapter, and the assembly was attached to a high vacuum manifold. After the reaction vessel had been evacuated, the suspension was allowed to slowly warm to room temperature with generation of B$_2$H$_6$. From a calibrated bulb, approximately 0.150 mmol of diborane was condensed into a NMR tube. Once the addition of diborane was completed, the NMR tube was flame sealed. ^{1}H and ^{11}B NMR spectra were initially taken at −5 °C, and then the temperature was gradually raised to 20 °C over 3 h. The reaction cleanly formed Cp*$_2$NbBH$_4$ and catecholborane, with ^{11}B spectra indicating 92% catecholborane (δ 28.4, d, J_{HB} = 193 Hz) and 8% boron decomposition product (δ 22.3, s).

6a + CO. A toluene-d_8 (0.75 mL) solution of **6a** (8.0 mg, 0.015 mmol) was placed in a NMR tube. The contents of the NMR tube were frozen with liquid nitrogen, and then the tube was evacuated. Approximately 1 atm of CO was admitted to the frozen contents of the tube, after which it was flame sealed. The reaction was followed

at 0 °C. Evaluation of ^{1}H spectral intensities resulted in a calculated half-life of 80 min.

6b + CO. A 9.0-mg (0.014 mmol) sample of tantalum complex was dissolved in 0.75 mL of toluene-d_8 and placed in a NMR tube. The contents were then frozen with liquid nitrogen, and the tube was evacuated. CO (approximately 1 atm) was admitted, after which the tube was flame sealed. The reaction was monitored at 70 °C and evaluation of ^{1}H spectral intensities resulted in a calculated half-life of 130 min. Integration of a final ^{11}B spectrum showed 73% free borane (δ 29, d, J_{HB} = 190 Hz) and 27% $B_2Cat'_3$ (δ 23, s). A final ^{1}H spectrum indicated the formation of $Cp^*_2TaH(CO)$[17] as the major Cp* product.

6a + C_2H_4. A 15-mg (0.028 mmol) sample of the niobium complex was dissolved in ~0.6 mL of toluene-d_8 and placed in a NMR tube. This tube was then frozen with liquid nitrogen and evacuated. Ethylene (~1 atm) was then admitted to the frozen contents of the NMR tube, which was then flame sealed. ^{1}H and ^{11}B NMR spectra were initially taken at 10 °C and increased to 40 °C over the course of the 3 h reaction time. The products of the reaction were $Cp^*_2NbH(C_2H_4)$ and free borane. Integration of the final ^{11}B spectrum showed 18% $EtBO_2C_6H_3$-4-^{t}Bu (δ 36.1, s), 74% of free borane (δ 28.8, d, J_{HB} = 190 Hz), and 8% of a boron decomposition product (δ 22.8, s).

6a + C_3H_6. A 15-mg (0.028 mmol) sample of niobium compound was dissolved in ~0.6 mL of toluene-d_8. This solution was placed in a NMR tube and frozen with liquid nitrogen, followed by evacuation of the gases. Approximately 1 atm of propylene was then admitted to the frozen contents of the NMR tube, after which it was flame sealed. Initial ^{1}H and ^{11}B NMR spectra (taken at 0 °C) showed the formation of $Cp^*_2NbH(C_3H_6)$ and free borane. However, as the reaction proceeded the concentration of the free borane diminished and the concentration of *n*-propylborane increased. After the 3 h reaction time, during which the temperature had been gradually raised to 40 °C and then lowered to 25 °C, a ^{11}B spectrum indicated clean conversion to *n*-propylborane (93%, δ 35.6, s) and a boron-containing decomposition product (7%, δ 22.2, s). A final ^{1}H spectrum revealed the presence of $Cp^*_2NbH(C_3H_6)$.

6a + H_2. A benzene-d_6 (~0.6 mL) solution of **6a** (15.0 mg, 0.028 mmol) was placed in a NMR tube. This solution was frozen with liquid nitrogen. Addition of ~1 atm of H_2 gas was preceeded by evacuation of the frozen NMR tube. ^{1}H and ^{11}B NMR spectra, initially taken at 20 °C and gradually raised to 50 °C over the 4 h reaction time, indicated formation of $Cp^*_2NbH_3$ and free borane. Integration of the final ^{11}B NMR spectrum showed 80% of free borane (δ 28.5, d, J_{HB} = 185 Hz) and 20% of the boron decomposition product, B_2Cat_3 (δ 22.2, s).

Crystal Structure Determination and Refinement for 16 and 17. Data were collected at 173 K on a Rigaku AFC6S diffractometer using Mo Kα radiation (λ = 0.71069 Å). Final unit cell parameters were obtained by least-squares refinement of 25 reflections that had been accurately centered. Three standard reflections were recorded after every 150 scans, with no significant change in intensity noted. The structures were solved by using SHELXL-86 in the teXsan[19] software package. Atomic coordinates and thermal parameters were refined F^2 data, using the full-matrix least-squares program, SHELXL-93.[20] All non-hydrogen atoms were refined by using anisotropic thermal parameters. All crystallographic computations were performed on Silicon Graphics Indigo computers.

Orange-red crystals of $Cp^*_2Nb(H_2BO_2C_6H_3$-3-^{t}Bu) (fw 539.7) were grown from a toluene/heptane solution cooled to −35 °C. The crystals were coated with Paratone-N, and a suitable crystal was selected and mounted on a glass fiber. Compound **16** crystallized in a triclinic crystal system with systematic absences indicating the space group $P\bar{1}$ (No. 2) with the following cell parameters: a = 9.923(3) Å, b = 12.109(4) Å, c = 13.588(4) Å, α = 97.74(2)°, β = 100.86(2)°, γ = 107.09(2)°, V = 1500.9(8) Å^3, Z = 2. Density(calculated) = 1.298 mg/cm^3. The 8555 independent reflections were collected between $4.0 \le 2\theta \le 60.0°$, using $\omega/2\theta$ scans.

All non-hydrogen atoms except one Cp* methyl carbon and the toluene solvent molecule were found by using SHELXS-86. DIRDIF WFOUR was used to extend and initially "refine" the structure. The toluene solvent molecule was found and modeled later to fit the difference map peaks. SHELXL-93 was used to refine the structure. The hydrogen atoms of each Cp* methyl group were calculated as two sets of half-occupancy positions, rotated initially about the C−C bond by 60° from each other, and refined with occupancy factors of x and $1 - x$ and with a common isotropic displacement parameter. Later, a single set of hydrogen atoms for each Cp* methyl group was placed at the occupancy-weighted average H positions. Restraints were applied separately to each methyl group to make all C−H distances the same, all H−H distances the same, and all C−C−H angles the same and to use a common isotropic displacement parameter. The hydrogen atoms of the boryl ring and its *tert*-butyl group were placed in calculated positions and refined independently without restraints. The toluene solvent molecule is disordered about an inversion center with both half-occupancy molecules coplanar and some atoms (e.g., C32 and C36*, etc.) nearly overlapping each other. The ring protons were restrained to lie 0.95 Å from their carbon atoms and equidistant from the two adjacent carbon atoms. The seven carbon atoms and the five ring hydrogen atoms of the toluene molecule were restrained to lie in a plane. The methyl hydrogen atoms were treated as the Cp* methyl hydrogens above. Full-matrix least-squares refinement on F^2 (8548 data, 181, restraints, 462 parameters) converged to give the following values: $R1$ = 0.0502, $wR2$ = 0.1220, GOF = 1.067 for $[I > 2\sigma(I)]$. For all data $R1$ = 0.0730 and $wR2$ = 0.1402. $R1 = \sum(F_o^2 - F_c^2)/\sum F_o^2$, $wR2 = [(w(F_o^2 - F_c^2)^2/\sum w(F_o^2)^2)]^{1/2}$, and GOF = $(\sum(|F_o^2| - |F_c^2|)/\sigma)/(n - m)$, where $w = 1/\sigma^2(F_o^2)$, n is the number of reflections used, and m is the number of variables.

Green crystals of $Cp^*_2NbBH_4$ (fw 377.7) were grown from a concentrated solution of heptane cooled to −35 °C. The crystals were coated with Paratone-N, and a suitable crystal was selected and mounted on a glass fiber. Compound **17** crystallized in a monoclinic crystal system with systematic absences indicating the space group $P2_1/c$ (No. 14) with the following cell parameters: a = 8.482(2) Å, b = 25.306(6) Å, c = 9.924 (3) Å, β = 113.84(2)°, V = 1948.39(9) Å^3, Z = 4. Density(calculated) = 1.298 mg/cm^3. The 3423 independent reflections were collected between $4.0 \le 2\theta \le 50.0°$, using ω scans. All non-hydrogen atoms were located in the solution found by SHELXS-86. Methyl hydrogens for the Cp* ligand were placed in calculated positions (0.95 Å), and their isotropic thermal parameters were allowed to ride on the parent carbon atoms. The hydrides were located in the difference-fourier map and were refined isotropically. Full-matrix least-squares refinement on F^2 (3402 data, 30 restraints, 335 parameters) converged to give the following values: $R1$ = 0.0455, $wR2$ = 0.1110, GOF =1.139 for $[I > 2\sigma(I)]$. For all data $R1$ = 0.1125 and $wR2$ = 0.1566. $R1 = \sum(F_o^2 - F_c^2)/\sum F_o^2$, $wR2 = [(w(F_o^2 - F_c^2)^2/\sum w(F_o^2)^2)]^{1/2}$, and GOF = $(\sum(|F_o^2| - |F_c^2|)/\sigma)/(n - m)$, where $w = 1/\sigma^2(F_o^2)$, n is the number of reflections used, and m is the number of variables.

Results and Discussion

Bercaw and co-workers have shown that olefin−hydride complexes in the group 5 bent-metallocene family can serve as models for olefin insertion into metal−hydride bonds. In these systems equilibrium between 16-electron intermediates, $Cp^*_2MCH_2CH_2R$ (R = H (**3**), CH_3 (**4**)), and the ground state olefin hydride structures, **1** and **2**, has been established by dynamic NMR experiments.[13,21] The fact that **1** and **2** form 18-electron, alkylcarbonyl complexes, $Cp^*_2M(CO)(CH_2CH_2R)$, in trapping reactions with CO illustrates the important role of the 16-electron alkyl intermediates to the reactivity of the olefin−hydride complexes. Although **1** and **2** generally react via these coordinatively unsaturated intermediates, the formation of a stable adduct between $Cp^*_2Ta(CH_2{=}CH_2)(H)$ and trimethylaluminum shows that the olefin ligand in the ground state complexes can interact with Lewis acids.[22] Hence, borane interactions with both the ground state olefin complexes (**1**, **2**) and the alkyl intermediates (**3**, **4**) are not unreasonable.

(19) TEXRAY Structure Analysis Package, SGI Version 1.8, Molecular Structure Corp., The Woodlands, TX, 1996.

(20) Sheldrick, G. M. University of Göttingen, Germany, 1993.

(21) (a) Green, M. L. H.; Sella, A.; Wong, L.-L. *Organometallics* **1992**, *11*, 2650−2659. (b) Green, M. L. H.; Wong, L.-L.; Sella, A. *Organometallics* **1992**, *11*, 2660−2668.

(22) McDade, C.; Gibson, V. C.; Santersiero, B. D.; Bercaw, J. E. *Organometallics* **1988**, *7*, 1−7.

Scheme 1

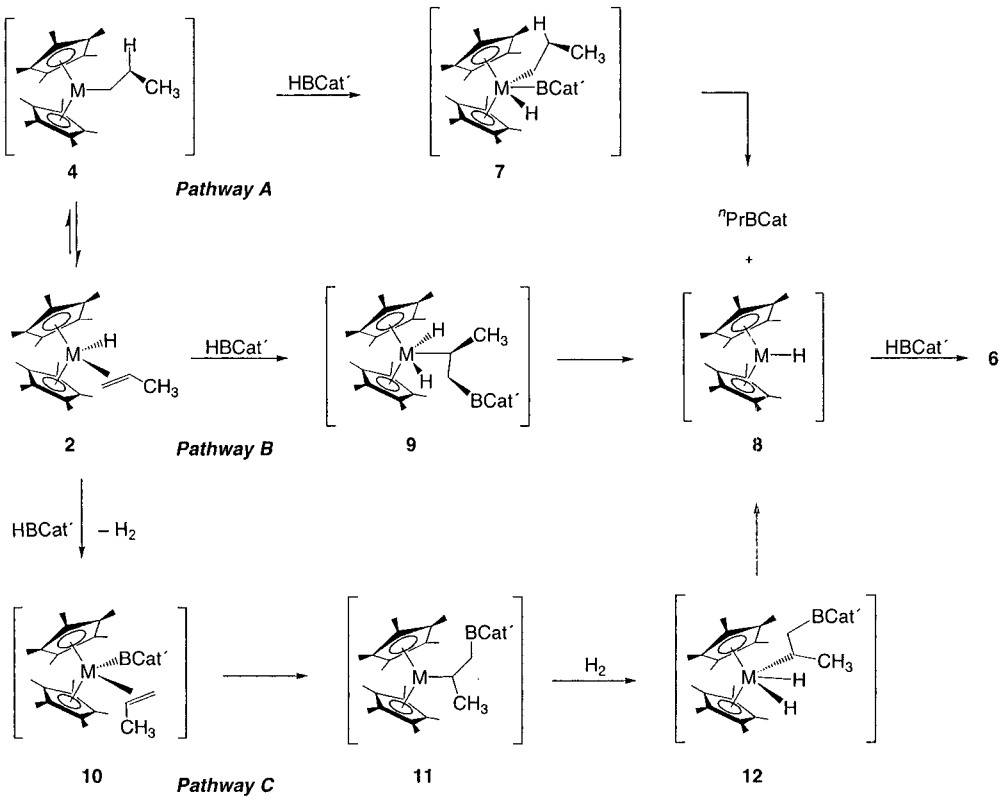

Compounds **1** and **2** reacted smoothly with 2 equiv of catecholborane (HBCat) to produce *endo*-Cp*$_2$M(H$_2$BCat) (M = Nb (**5a**), Ta (**5b**)) and the alkylborane products EtBCat and ^{n}PrBCat (eq 1).[23] The analogs *endo*-Cp*$_2$M(H$_2$BCat′) (M =

$$\mathrm{Cp^*_2M(CH_2{=}CH(R))(H) + 2HBCat \rightarrow Cp^*_2M(H_2BCat) + RCH_2CH_2BCat} \quad (1)$$

$$\mathrm{R = H, CH_3;\ M = Nb, Ta}$$

Nb (**6a**), Ta (**6b**)) were similarly prepared from HBO$_2$C$_6$H$_3$-4-^{t}Bu (HBCat′), in which the ^{t}Bu substituent provides a convenient NMR handle for monitoring catecholate species in solution. Since the propylene compounds reacted more readily than their ethylene counterparts, compounds **5** and **6** were most conveniently prepared from **2a** and **2b**. When the reactions were monitored by NMR, intermediates were not observed, and addition of 1 equiv of HBCat′ resulted in a 50% conversion of **2a** and **2b** to compounds **6a** and **6b**, respectively. The ^{11}B chemical shifts for the H$_2$BCat moiety are similar to those observed in the related cyclopentadienyl counterparts, and high-field ^{1}H NMR resonances that are typical for group 5 decamethylmetallocene hydrides are observed.

Some potential mechanisms that could account for the observed products from the reaction of the propylene complexes (**2**) with HBCat′ are shown in Scheme 1. In Pathway A, the reaction proceeds via the aforementioned alkyl hydride intermediates. After the olefin insertion step, catecholborane oxidatively adds to **4** to generate a boryl intermediate, **7**. Reductive elimination of the organic borane from this putative species generates monohydride **8**. Intermediate **8** is common to all three mechanisms, and compound **6** forms when **8** is trapped with HBCat′. Alternatively, σ-bond metathesis between **4** and HBCat′ could generate **8** directly, circumventing intermediate **7**. Pathway B invokes ring-opening of the metallacyclopropane similar to that proposed in reactions of Ti olefin complexes.[11g,12] Reductive elimination of ^{n}PrBCat from the dihydride complex (**9**) generates the common hydride intermediate. In Pathway C, metathesis between metal−hydride and B−H bonds generates a boryl−olefin intermediate **10** with loss of H$_2$.[24] Trapping of the product of olefin insertion into the metal−boron bond **11** with H$_2$ gives a dihydride intermediate **12** that can reductively eliminate alkylborane to yield **8**.

These mechanisms all assume that the metal center mediates B−C bond formation. This assumption can be dangerous since a common problem in early metal systems is the tendency for the metal to effect disproportionation of HBCat to BH$_3$ and B$_2$Cat$_3$.[5k,11b] Thus, hydroboration by transient BH$_3$ can masquerade as hydroboration where B−C bond formation occurs at the metal center. Although traces of B$_2$Cat$_3$ were observed, hydroboration by BH$_3$ did not seem likely in these systems because B^{n}Pr$_3$ was not observed in the reaction mixtures. Nevertheless, participation of BH$_3$ can be definitively addressed by labeling experiments (vide infra).

Efforts to apply a rigorous kinetic analysis were complicated by irreproducibility in rate constants measured under pseudo-first-order conditions of high borane concentration. Despite these inconsistencies, two significant variations in rate were observed. First, the Nb complexes reacted more rapidly than their Ta analogs. Second, observed rates for the propylene complexes (**2a,b**) were faster than those for their ethylene counterparts (**1a,b**). Based on the fact that propylene insertion into the M−H is faster than insertion of ethylene,[13] it is tempting to argue that this qualitative disparity in rates is consistent with the proposed mechanism. However, this is misleading and can

(23) This approach has recently been reported as a route to preparing bis(silyl)niobocene complexes: Nikonov, G. I.; Kuzmina, L. G.; Lemenovskii, D. A.; Kotov, V. V. *J. Am. Chem. Soc.* **1995**, *117*, 10133−10134.

(24) Boryl synthesis from metathesis of B−H and Nb−H bonds has precedent: Hartwig, J. F.; De Gala, S. R. *J. Am. Chem. Soc.* **1994**, *116*, 3661−3662.

Scheme 2

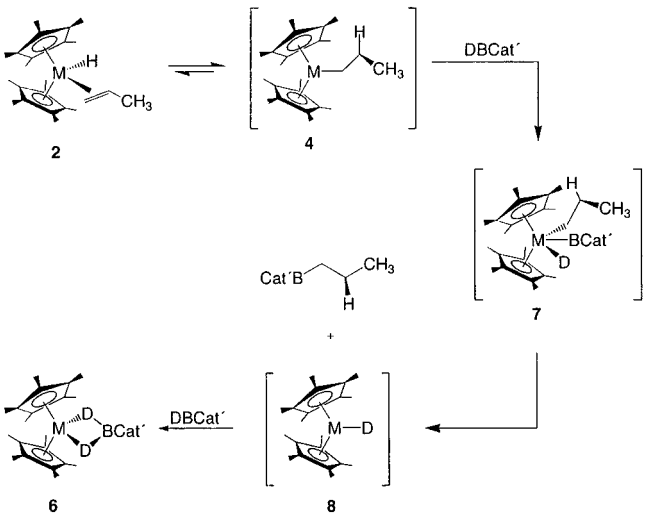

only be confirmed if k_{obs} approaches a limiting value (the rate of olefin insertion) at high borane concentration.

Since rate constant variations precluded detailed analyses, our mechanistic hypotheses were tested by isotopic labeling and trapping experiments. The reaction of **2a** with catecholborane-*d* provided considerable information with regard to the pathways in Scheme 1. When the reactions were monitored by NMR, scrambling between the deuterated borane and hydride or olefin protons in the olefin complexes was not observed. Thus, reversible B−H/M−H exchange by interaction between catecholborane and **1** or **2** does not occur. Some important conclusions can be drawn from the following observation: *The nascent alkylborane products show no deuterium incorporation*. On the basis of this result, scenarios where the organoborane products arise from hydroboration of free olefins by DBCat or BD_3, generated from disproportionation of DBCat, can be excluded. The isotopic labeling experiment also bears strongly on the mechanistic possibilities in Scheme 1. For pathways B and C, deuterated borane products would be expected given that eliminations from d_1-dihydride intermediates are common to both mechanisms.[25]

The fate of the deuterium label is revealed by ^{2}H and ^{1}H NMR spectra. For the Nb complex, **6a**, deuterium is incorporated at niobium−deuteride and Cp* methyl positions in a 90:10 ratio (^{2}H NMR). This is also confirmed by integrating the methyl resonances of the d_0, d_1, and d_2 isotopomers in the ^{1}H NMR spectra (vide infra). Label scrambling in the Nb compound is not surprising as deuterium incorporation at the Cp* methyl positions has been observed when $Cp^*_2NbH_3$ is treated with D_2. This scrambling was attributed to reversible C−H activation of the Cp* methyl group in the intermediate hydride, Cp^*_2NbD (**8**).[16] Similar participation of **8** in the present reaction could account for scrambling of the isotopic label in **6a**. When crystalline samples of labeled **6a** are stored at room temperature for extended periods, the isotopic label at the hydride position gradually diminishes and incorporation at the cyclopentadienyl methyl positions is enhanced (^{1}H, ^{2}H NMR). For the Ta propylene−hydride complex, reaction with DBCat′ generates **6b**-d_2. In this case, deuterium incorporation was only observed at the metal deuteride positions. The experimental results from the labeling experiment are most consistent with the mechanism in pathway A as the deuterium label should be confined to the metal complexes **6a** and **6b**. Scheme 2 shows the positions where deuterium incorporation is expected based on this operating mechanism.

As a final test for hydroboration by X_2BH species, the reaction of **2a** with HBCat′ was performed in the presence of excess cyclooctene. The rates for uncatalyzed hydroboration of cyclooctene and α-olefins by BH_3 are competitive.[26] Thus, any B−C bond forming pathway that does not occur at the metal should give appreciable quantities of cyclooctene hydroboration products. In this case, **2a** is converted to **6a** and ^{n}PrBCat′ is the primary alkylborane product observed. This result, coupled with the isotopic labeling experiments, conclusively demonstrates that B−C bond formation occurs at the metal center.

"Catecholateboryl" complexes of the group 5 transition elements are rare. Compounds **5** and **6** are the first in this family supported by pentamethylcyclopentadienyl ligands, and they join the recently reported examples *endo*-$Cp_2Nb(H_2BCat)$ (**13**),[24] *endo*-$Cp_2TaH_2(BCat)$ (**14**), and *exo*-$Cp_2TaH_2(BCat)$ (**15**).[27] For *endo*-$Cp'_2MH_2BX_2$ complexes, three limiting forms that can be used to describe H_2BX_2 ligation include d^0 boryl (**A**), d^2 borohydride (**B**), and d^2 agostic borane (**C**) structures.[28] Chemical shift perturbations on isotopic substitution (vide infra) and crystallographic data support interactions between boron and the hydride coligands in **13** and the central hydride ligand in **15**. Compound **14** is the only definitive example of structure **A** as B−H interactions are not confirmed by crystallographic and spectroscopic data.

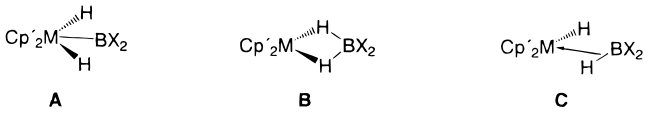

Given the steric and electronic differences between Cp and Cp* ligands, M−B or B−H interactions in **6a** could differ significantly from those in **13**. Attempts to grow single crystals of **5a** and **6a** were not successful; however, suitable single crystals of the compound *endo*-$Cp^*_2Nb(H_2BO_2C_6H_3$-3-^{t}Bu) (**16**), derived from reaction of **2a** with $HBO_2C_6H_3$-3-^{t}Bu, were grown from a toluene/heptane solution. The molecular structure for **16** reveals some interesting features (Figure 1a). The structural parameters for the "boryl" fragment differ significantly from its Cp counterpart. Most notably, the Nb−B distance of 2.348(4) Å is considerably longer than the Nb−B distance of 2.292(5) Å in **13**. This elongation in the Nb−B vector, in addition to the positions of the hydride ligands (vide infra), suggests that **16** might be more accurately described as a borohydride complex. The best benchmark for comparison in the decamethylmetallocene system is the borohydride complex, $Cp^*_2Nb(BH_4)$ (**17**).[17,29] Since **17** had not been crystallographically characterized, we determined its structure. For compound **17** (Figure 1b), the Nb−B bond length of 2.35(1) Å is identical, within experimental error, to that observed in **16**.

Geometric parameters for the hydride ligands are crucial for discriminating between boryl and borohydride structures. Although the uncertainties in hydride positions determined by X-ray diffraction are large when a hydride is bonded to a heavy element, useful information can be obtained if the data are of sufficient quality and proper care is exercised in their interpreta-

(25) If dihydride intermediates are involved, the failure to detect deuterated borane products would require that $k_H/k_D > 50$.

(26) Suzuki, A.; Dhillon, R. S. *Top. Curr. Chem.* **1986**, *130*, 23−88.

(27) Lantero, D. R.; Motry, D. H.; Ward, D. L.; Smith, M. R., III. *J. Am. Chem. Soc.* **1994**, *116*, 10811−10812.

(28) (a) Calderon, J. L.; Cotton, F. A.; Shaver, A. *J. Organomet. Chem.* **1972**, *42*, 419−427. (b) Cotton, F. A.; Jeremic, M.; Shaver, A. *Inorg. Chim. Acta* **1972**, *6*, 543−551.

(29) An Nb−B distance of 2.26 Å has been reported in $Cp_2Nb(BH_4)$. The uncertainty in the Nb−B distance from this study is 0.06 Å: Kirillova, N. I.; Gusev, A. I.; Struchkov, Y. T. *J. Struct. Chem. USSR* **1974**, *15*, 622−624.

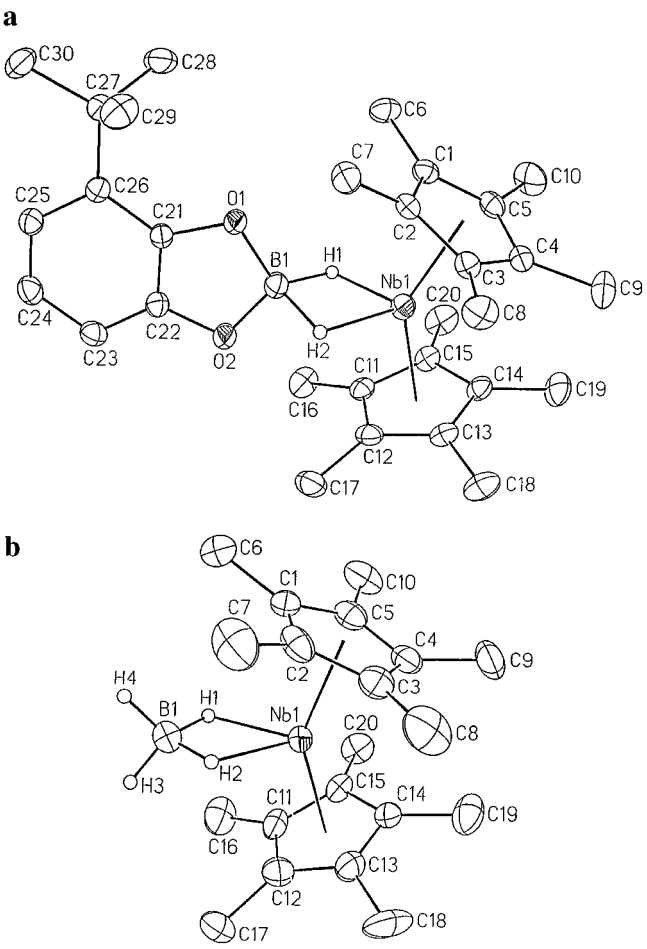

Figure 1. ORTEP diagrams of (a) *endo*-$Cp^*_2Nb(H_2BO_2C_6H_3$-3-^{t}Bu) (**16**) and (b) $Cp^*_2Nb(H_4)$ (**17**). Ellipsoids represent 30% probability for electron density.

tion. After the refinement for the non-hydrogen atom positions in **16** and **17** had converged, difference maps revealed Nb−H peaks in chemically reasonable positions. These atom positions were added to the models, and in both cases they refined normally. To ensure that these refined positions were not artifacts of residual electron density at the Nb center, difference maps were calculated by fixing the non-hydrogen atom positions and using low-angle data ($4 < 2\theta < 30$).[30] Difference Fourier maps (see Supporting Information) clearly show maxima at the same positions as found by refining the hydride ligands. Thus, the hydride positions do not appear to be artifacts of refinement. Table 1 contains the metrical parameters for the $Nb(H_2BX_2)$ moieties in **13**, **16**, and **17**.

The H−Nb−H angle in **16** more closely resembles that in **17** (58(3)°) than $\angle H_{exo}-Nb-H_{exo}$ in Cp_2NbH_3 (126 (3)°),[31] and the B−H distances in **16** lie near the mean found for the corresponding distances in **13** and **17**. The B−H contacts are longer than those typically found in borohydride complexes or diborane; however, similar B−H distances have been reported for hydrides that bridge boron centers bearing N or O substituents.[32,33] Thus, **16** may be best described as an HBCat′ adduct of "Cp^*_2NbH". While the hydride ligands in **13** and **17** are symmetrically disposed, the refined positions in **16** are asymmetric. We hesitate to attach undue significance to this observation, although contributions from an agostic borane structure should not be dismissed given the precedent established by Cotton and co-workers[28] and the recently reported structure of $Cp_2Ti(\eta^2$-HBCat$)_2$.[34] In any event, the metrical data for the hydride ligands and the long Nb−B distance are clearly consistent with pronounced Nb(III) character in **16** relative to its Cp counterpart, compound **13**. Of the structurally characterized compounds with the formulation $Cp_2Nb(H_2BX_2)$, the MH_2BX_2 linkage in **16** most closely resembles the complex that results from the reaction between Cp_2NbH_3 and 9-BBN, $Cp_2Nb(H_2BC_8H_{14})$ (**18**).[24]

The recently synthesized boryl compounds in these group 5 metallocene systems establish a database for assessing relationships between structural and spectroscopic features for boryl and borohydride complexes. Relevant NMR and IR data for $Cp'_2MH_2BX_2$ derivatives and related hydride complexes are given in Table 2.[15−17,24,27,35−38] At first glance, the ^{11}B chemical shifts appear to correlate with the boryl and borohydride character. For example, *endo*-Cp_2TaH_2(BCat) and *endo*-$Cp^*_2TaH_2$(BCat) exhibit low-field chemical shifts and their structural and spectroscopic data are more consistent with d^0 boryl structures. Meanwhile, in parent and alkyl-substituted d^2 borohydride complexes, the ^{11}B nuclei resonate at higher field. However, the ^{11}B data for $Cp_2Nb(H_2BCat)$ and $Cp^*_2Nb(H_2BCat)$ clearly illustrate the limitations of empirical correlations of chemical shift to boryl and borohydride bonding modes. This is not surprising as the observed chemical shift results from several contributing factors. While boryl and borohydride complexes typically exhibit a ^{11}B resonance between 40 and 75 ppm, subtle structural variations cannot be reliably correlated to chemical shift.

For compound **13**, Hartwig and co-workers attributed large perturbations in the hydride chemical shifts to rapid chemical equilibrium between d^0 borylhydride (**A**) and d^2 dihydridoborate (**B**) structures.[24] For compounds **6a**-d_{0-2}, we observe perturbations in the hydride resonances of similar magnitude to those in **13**-d_{0-2}, and the hydride/deuteride resonance shifts to higher field as D is substituted for H. For the tantalum congener, **6b**, ^{1}H NMR spectra reveal only minor perturbations in the hydride resonances to the d_0 and d_1 isotopomers as was observed for the Cp analogue, **14**.

For the sake of the current discussion, it is important to consider the origins of these abnormally large perturbations and their bearing on potential solution structures. Isotopic perturbations for ^{1}H resonances in partially deuterated hydrocarbons are well-documented.[39] For example, the methyl resonance in toluene-d_α lies 0.015 ± 0.002 ppm upfield of the same resonance in toluene.[40] The interpretation of the large isotopic perturbations in $Cp'_2Nb(H_2BCat)$ is more complex. By using the simple harmonic oscillator approximation, vibrational zero-point energies can be expressed as a function of the force constant and reduced mass. By virtue of deuterium's larger mass, the zero-point energies in deuterium isotopomers of **A** and **B** will be

(30) The scattering factor for hydrogen decays rapidly as $\sin(\theta/\lambda)$ increases. Thus, hydride positions can be more reliably located from low-angle data: La Placa, S. J.; Ibers, J. A. *Acta Crystallogr.* **1965**, *18*, 511−519.

(31) Wilson, R. D.; Koetxle, T. F.; Hart, D. W.; Kvick, Å.; Tipton, D. L.; Bau, R. *J. Am. Chem. Soc.* **1977**, *99*, 1775−1781.

(32) Müller, G.; Krüger, C. *Acta Crystallogr.* **1986**, *C42*, 1856−1859.

(33) Yalpani, M.; Köster, R.; Boese, R. *Chem. Ber.* **1993**, *126*, 565−570.

(34) Hartwig, J. F.; Muhoro, C. N.; He, X. *J. Am. Chem. Soc.* **1996**, *118*, 10936−10937.

(35) Antiñolo, A.; Fajardo, M.; Otero, A.; Royo, P. *J. Organomet. Chem.* **1983**, *246*, 269−278.

(36) Green, M. L. H.; Wong, L. L. *J. Chem. Soc., Chem. Commun.* **1989**, 571−573.

(37) Tebbe, F. N.; Parshall, G. W. *J. Am. Chem. Soc.* **1971**, *93*, 3793−3795.

(38) Green, M. L. H.; McCleverty, J. A.; Pratt, L.; Wilkinson, G. *J. Chem. Soc.* **1961**, 4854−4859.

(39) Bovey, F. A. *Nuclear Magnetic Resonance Spectroscopy*, 2nd ed.; Academic Press: San Diego, 1988; p 141.

(40) Tiers, G. V. D. *J. Chem. Phys.* **1958**, *29*, 963−964.

Table 1. Geometric Parameters for *endo*−$Cp'_2Nb(H_2BX_2)$ Compounds

compd	Nb−B	Nb−H	B−H	H−Nb−H	H−B−H
endo-$Cp_2Nb(H_2BCat)$ (**13**)	2.292(5)	1.62(4) 1.58(5)	1.69(4) 1.62(5)	92(2)	
endo-$Cp^*_2Nb(H_2BO_2C_6H_3$-3-^{t}Bu) (**16**)	2.348(4)	1.86(4) 1.63(4)	1.36(4) 1.46(4)	73(2)	95(2)
$Cp^*_2Nb(BH_4)$ (**17**)	2.35(1)	1.88(7) 1.79(8)	1.17(7) 1.16(8)	58(3)	100(5)

Table 2. Spectroscopic Data for $Cp'_2M(H_2BX_2)$ and Cp'_2MH_3 Compounds

compd	^{11}B NMR[a]	ν_{BHM} (cm^{-1})[b]	ν_{MH} (cm^{-1})[b]
endo-$Cp^*_2Nb(H_2BCat)$ (**5a**)	60.2	1653	
endo-$Cp^*_2Nb(H_2BO_2C_6H_3$-4-*t*Bu) (**6a**)	60.0	1653	
endo-$Cp^*_2Nb(H_2BO_2C_6H_3$-3-*t*Bu) (**16**)	60.9	1649	
endo-$Cp_2Nb(H_2BCat)$[c] (**13**)	59	1742, 1675[d]	
endo-$Cp^*_2Ta(H_2BCat)$ (**5b**)	73.5	1774, 1709	
endo-$Cp^*_2Ta(H_2BO_2C_6H_3$-4-*t*Bu) (**6b**)	72.7	1767, 1720	
endo-$Cp_2Ta(H_2BCat)$[e] (**14**)	70.0	1768	
exo-$Cp_2Ta(H_2BCat)$[e] (**15**)	64.7	1771, 1703	
$Cp_2Nb(H_2BC_8H_{14})$[c] (**18**)	57	1605	
$Cp^*_2Nb(BH_4)$[f] (**17**)	43.4	1728, 1620	
$Cp_2Nb(BH_4)$[g]	40.5	1745, 1628	
$Cp_2Ta(BH_4)$[h]		1882−1860	
$CpCp^*Ta(BH_4)$[i]	47.2	1747, 1621	
$Cp^*_2NbH_3$f			1747, 1695
Cp_2NbH_3[j]			1710
$Cp^*_2TaH_3$[k]			1750, 1720
Cp_2TaH_3[l]			1735

[a] ^{11}B spectra were recorded in benzene-d_6 and are referenced to an external $BF_3{\cdot}OEt_2$ standard. [b] Recorded as Nujol mulls unless otherwise indicated. [c] Reference 24. [d] KBr pellet. [e] Reference 27. [f] Reference 17. [g] Reference 15. [h] Reference 35. [i] Reference 36. [j] Reference 37. [k] Reference 16. [l] Reference 38.

lower than their hydride counterparts. More importantly, if the force constants for the hydride vibrational modes in **A** and **B** are not identical, the energy separations $\Delta G°$(**A**-d_0) − $\Delta G°$(**B**-d_0) and $\Delta G°$(**A**-d_1) - $\Delta G°$(**B**-d_1) will be different, and deuteration will shift the equilibrium between structures **A** and **B**. If the equilibrium is rapid on the NMR time scale, the observed hydride chemical shift will be a weighted average of the chemical shifts for the hydride ligands in the limiting structures, and the isotopic perturbation of the equilibrium between **A** and **B** will lead to a shift in the hydride/deuteride resonance.[41] The fact that the hydride/deuteride resonances shift to higher field with each deuterium substitution excludes any equilibrium between degenerate structures. Although equilibrium between **A** and **B** is an appealing explanation for the observed isotopic perturbation, other nondegenerate equilibria could account for these spectroscopic features. Some potential alternatives are shown in Scheme 3.[42] Lastly, the equilibria responsible for perturbations in compounds **16** and **13** need not be analogous. The large chemical shift perturbations provide strong evidence for equilibrium between structural extremes in these systems; however, the structures that participate in the equilibria cannot be unambiguously assigned from these data.

Attempts to crystallographically characterize **6b** have not been successful; however, "normal" isotopic perturbations for the hydride/deuteride chemical shifts in **6b**-d_{0-2} argue against rapid structural equilibration. Although structural differences for the Nb Cp and Cp* compounds clearly illustrate the pitfalls inherent

Scheme 3

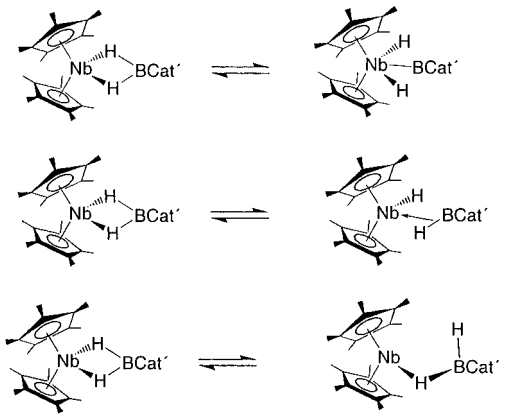

in assigning structural types based on spectroscopic similarities, the spectroscopic data for **6b** do not support significant B−H interactions. Thus, **6b** most likely adopts a d^0 boryl structure similar to its Cp counterpart, **14**.

Vibrational spectroscopy is useful for identifying three-center, two-electron bonding in borohydride and related agostic complexes.[43−48] With several structurally characterized compounds in hand, the utility of vibrational spectroscopy for

(41) The difference in chemical shifts between isotopomers is temperature dependent. At 20 °C, $\Delta\delta$ between Cp_2*Nb(*H*$_2$BCat′) and Cp_2*Nb(*H*DBCat′) and Cp_2*Nb(H*D*BCat′) and Cp_2*Nb(*D*$_2$BCat′) is 0.42 and 0.43 ppm, respectively. At −60 °C, $\Delta\delta$ between Cp_2*Nb(*H*$_2$BCat′) and Cp_2*Nb(*H*DBCat′) and Cp_2*Nb(H*D*BCat′) and Cp_2*Nb(*D*$_2$BCat′) is 0.54 and 0.51 ppm, respectively.

(42) Intermediacy of $Cp^*_2Nb(\eta^1$-$H_2BCat')$ could account for the observed scrambling between Cp* methyl hydrogen and Nb−D positions in solid samples of **6a**; however, rapid HBCat′ elimination prevents evaluation of intramolecular processes.

(43) Nakamoto, K. *Infrared and Raman Spectra of Inorganic and Coordination Compounds*; 4th ed.; Wiley-Interscience: New York, 1986.

(44) Marks, T. J.; Kennelly, W. J. *J. Am. Chem. Soc.* **1975**, *97*, 1439−1443.

(45) Strong evidence has been presented for three-center, two-electron bonding interactions in $[H_2B(3,5\text{-}Me_2Pz)_2](C_7H_7)(CO)_2Mo$ in solution[28a] and in the solid state.[28b] Perturbations in ν_{BH} were not reported; however, it is interesting to note that only one BH stretch is observed in IR spectra for these compounds instead of the two stretches normally observed in bispyrazolylborate complexes: Trofimenko, S. *Inorg. Chem.* **1970**, *9*, 2493−2499.

(46) Kubas, G. J. *Acc. Chem. Res.* **1988**, *21*, 120−128.

(47) Brookhart, M.; Green, M. L. H. *J. Organomet. Chem.* **1983**, *250*, 395−408.

Scheme 4

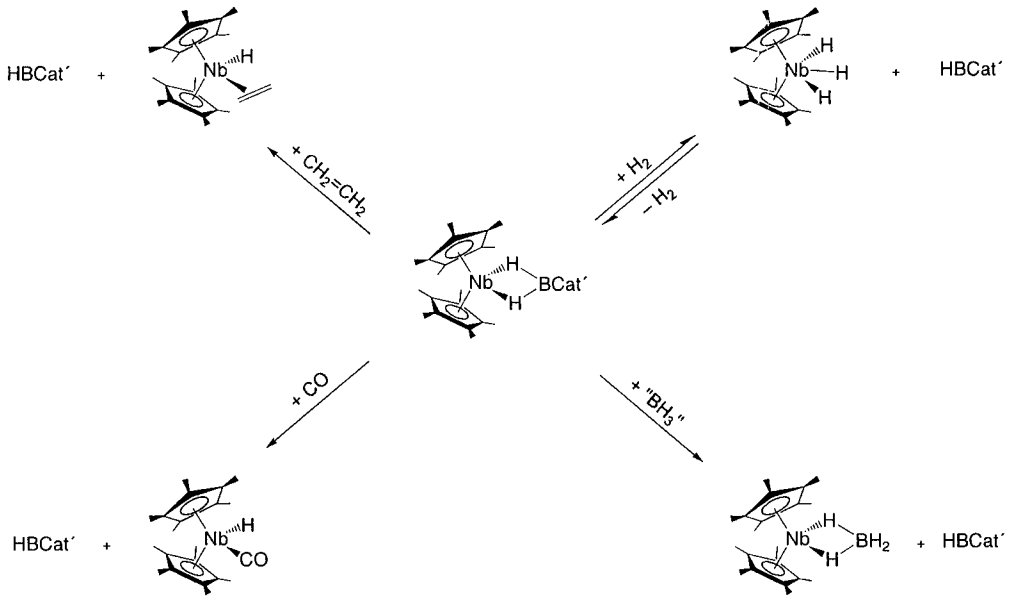

identifying more subtle variations in ligation can be assessed. From similar stretching frequencies for terminal hydride stretches in $Cp^*_2NbH_3$ and bridging borohydride vibrations in $Cp^*_2NbBH_4$, it is apparent that boryl/hydride and borohydride structures cannot be distinguished on the basis of IR data. With respect to agostic borane structures, ν_{BH} can be estimated to lie within a broad frequency range from 2200 to 1600 cm^{-1} by considering decreases in ν_{EH} observed upon coordination of other E−H bonds (E = H, C, Si) to metal centers. A high-frequency ν_{BH} mode could be correlated to an agostic borane structure; however, assignments for lower frequency modes observed for the compounds in this study are ambiguous since this portion of the window overlaps regions typical for stretching frequencies in borohydride and metal−hydride complexes.

Unfortunately, structures of *endo*-$Cp_2M(H_2BX_2)$ complexes cannot be unambiguously assigned from their NMR and IR spectra. In some cases spectroscopic data can provide information regarding interactions between boron and hydride coligands; however, we hesitate to attach undue significance to these observations since the reactivity of compounds where spectroscopic similarities are striking can differ dramatically.

In marked contrast to other catecholate-substituted group 5 boryl/borohydride complexes, **6a** exhibits clean reaction chemistry with various small molecules (Scheme 4) that is reminiscent of $Cp_2M(BH_4)$ complexes (M = Nb,[15,49] Ta[35]). The unifying feature for the reactions in Scheme 4 is elimination of HBCat′ from **6a** under mild conditions. Some details of the reactions shown in Scheme 4 merit comment. The reaction with ethylene is interesting, as extrusion of HBCat′ (observed by ^{11}B NMR) is accompanied by regeneration of the olefin−hydride complex **1a** that served as the starting point for synthesis of the boryl complex. On further heating, the liberated borane is converted to EtBCat′. As this result would suggest, solutions of **6a** catalyze olefin hydroboration.

Compound **6a** also reacts with other two-electron ligands. In each case, elimination of HBCat′ formally precedes trapping of "Cp^*_2NbH" by oxidative-addition or coordination of the substrate in question. For example, **6a** reacts with H_2 to generate $Cp^*_2NbH_3$ and HBCat′ under mild conditions. A reasonable mechanism involves B−H elimination to generate "Cp^*_2NbH", which is trapped by H_2. For the reaction between **6a** and D_2, HBCat′ is the initial elimination product as judged by ^{11}B NMR. Thus, elimination of the metal-bound hydride is rapid with respect to deuterium scrambling. As the reaction proceeds, DBCat′ is produced from the equilibrium between $Cp^*_2NbH_{3-x}D_x$ and HBCat′. Related reactions of **6a** with CO and B_2H_6 generate the Nb(III) complexes $Cp^*_2NbH(CO)$ and $Cp_2{}^*Nb(BH_4)$ with elimination of HBCat′. For these species, HBCat′ elimination is irreversible as **6a** cannot be regenerated by addition of HBCat′ to $Cp^*_2NbH(CO)$ or $Cp_2{}^*Nb(BH_4)$ under thermal conditions. In the elimination reactions outlined, traces of B_2Cat_3 (typically <10% by ^{11}B integration) are formed in these systems. We have not been able to pinpoint the source(s) responsible for this degradation.

$Cp^*_2Nb(H_2BCat')$ (**6a**) also eliminates borane more readily than does $Cp^*_2Nb(BH_4)$ (**17**). This difference in reactivity parallels related chemical behavior of BH_3 and HBCat. While HBCat exists as a monomer, the barrier for dissociation of B_2H_6 into two BH_3 fragments is considerable.[50] Thus, if the barrier for borane elimination from **6a** and **17** is also sensitive to borane heteroatom substitution, a lower activation energy would be expected for **6a** relative to **17**.

The tantalum analog, compound **6b**, reacts sluggishly when compared to its Nb cousin, as illustrated by the reactions of **6a** and **6b** with CO that generate HBCat′ and the carbonyl complexes $Cp^*_2Nb(H)CO$ and $Cp^*_2Ta(H)CO$, respectively. For **6a**, the reaction proceeds with a half-life of 80 min at 0 °C, while the corresponding reaction for **6b** has a half-life of 130 min at 70 °C. The difference in reactivity between **6a** and **6b** would be conveniently explained if **6b** is a Ta(V) boryl complex. In this case a higher barrier for reductive elimination of HBCat′ would be expected for **6b** relative to the Nb(III) species, **6a**, since borane elimination from a d^0 boryl complex requires a formal two-electron reduction of the metal center. The observation that other niobocene and tantalocene MH_2BCat compounds

(48) Spaltenstein, E.; Palma, P.; Kreutzer, K. A.; Willoughby, C. A.; Davis, W. M.; Buchwald, S. L. *J. Am. Chem. Soc.* **1994**, *116*, 10308−10309.

(49) Otto, E. E. H.; Brintzinger, H. H. *J. Organomet. Chem.* **1978**, *148*, 29−33.

(50) A dissociation enthalpy of 36.0 ± 3.0 kcal/mol has been measured for diborane.[50a] Computational methods predict a similar barrier for this reaction:[50b] (a) Fehlner, T. P.; Mappes, G. W. *J. Phys. Chem.* **1969**, *73*, 873−882. (b) Stanton, J. F.; Bartlett, R. J.; Lipscomb, W. N. *Chem. Phys. Lett.* **1987**, *138*, 525−530.

with significant M(V) character do not readily eliminate borane is consistent with this notion.

Conclusions

The olefin complexes **1** and **2** serve as well-defined models for investigating metal-mediated hydroboration. Isotopic labeling and deuterium trapping experiments strongly support a mechanism where B−C bond formation results from reaction of borane reagent with the 16-electron alkyl intermediates $Cp^*_2MCH_2CH_2R$. Significantly, hydroboration by transient BH_3 is not observed under stoichiometric or catalytic conditions. In contrast to the chemistry observed for $Cp^*_2Ti(\eta^2\text{-}CH_2{=}CH_2)$ and related Ti olefin complexes, isotopic labeling experiments preclude borane attack on the olefin ligands in the ground state complexes **1** and **2**. Despite their disparate olefin borylation products, the reactivity of $Cp^*_2Ti(CH_2{=}CH_2)$ and $Cp^*_2M(CH_2{=}CH(R))(H)$ with borane reagents is linked by a common feature. In both cases, interactions of B−H bonds with M−C bonds in coordinatively unsaturated, 16-electron complexes/intermediates most likely trigger B−C bond formation. The postulated mechanism for hydroboration of the olefin ligands in **1** and **2** is similar to those proposed for lanthanide and zirconium systems. Although B−H oxidative addition is precluded in lanthanide systems,[10] a borohydride resting structure for lanthanide catalysts is not unreasonable given the structure of **16**.

While boryl M(V) structures appear to be major contributors in other catecholateboryl compounds, *endo*-$Cp^*_2Nb(\eta^2\text{-}H_2\text{-}BO_2C_6H_3\text{-}3\text{-}^tBu)$ is better described as an Nb(III) complex. The structural parameters are consistent with its formulation as a borohydride complex, or an $HBO_2C_6H_3\text{-}3\text{-}^tBu$ adduct of "Cp^*_2NbH". In contrast to other group 5, metallocene catecholateboryl complexes, $Cp^*_2Nb(H_2BCat')$ readily eliminates HBCat′. The differences in reactivity can be rationalized by considering the changes in oxidation state that accompany extrusion of borane for these species. The formal oxidation state of the metal is unchanged for elimination from the decamethylniobocene complexes, whereas borane elimination from M(V) boryl complexes requires a two-electron reduction in the formal oxidation state of the metal. Thus, the disparities in rates for HBCat elimination from group 5 metallocene boryl/borohydride species are most likely related to their structures.

The facile elimination of HBCat′ from **6a** is the key to its catalytic activity. While hydrocarbon activation and elimination have been well studied, considerably less is known for analogous reactivity of B−H bonds.[5aik,7,51,52] Since thermal chemistry is clean and deuterium isotopomers can be readily prepared, this system is particularly well-suited for studying the factors that influence elimination of B−H bonds from transition metal centers. We are currently investigating the mechanistic details of borane elimination from these compounds, and are exploring reactivity of related olefin−hydride complexes.

Acknowledgment. The NMR equipment was provided by the National Science Foundation (CHE-8800770) and the National Institutes of Health (1-S10-RR04750-01). We thank the administrators of the ACS Petroleum Research Fund, the Exxon Educational Foundation, and the National Science Foundation (CHE-9520176) for support of this work.

Supporting Information Available: Tables of atomic coordinates, thermal parameters, and bond distances and angles for **16** and **17** and electron density maps used in locating hydride positions in **16** and **17** (46 pages). See any current masthead page for ordering and Internet access instructions.

JA970639B

(51) For related additions of B−H bonds to Rh see: (a) Baker, R. T.; Ovenall, D. W.; Harlow, R. L.; Westcott, S. A.; Taylor, N. J.; Marder, T. B. *Organometallics* **1990**, *9*, 3028−3030. (b) Westcott, S. A.; Taylor, N. J.; Marder, T. B.; Baker, R. T.; Jones, N. L.; Calabrese, J. C. *J. Chem. Soc., Chem. Commun.* **1991**, 304−305. (c) Baker, R. T.; Calabrese, J. C.; Westcott, S. A.; Nguyen, P.; Marder, T. B. *J. Am. Chem. Soc.* **1993**, *115*, 4367−4368.

(52) For oxidative additions of B−H bonds to Ir see: (a) Baker, R. T.; Ovenall, D. W.; Calabrese, J. C.; Westcott, S. A.; Taylor, N. J.; Williams, I. D.; Marder, T. B. *J. Am. Chem. Soc.* **1990**, *112*, 9399−9400. (b) Knorr, J. R.; Merola, J. S. *Organometallics* **1990**, *9*, 3008−3010. (c) Westcott, S. A.; Marder, T. B.; Baker, R. T.; Calabrese, J. C. *Can. J. Chem.* **1993**, *71*, 930−936. (d) Cleary, B. P.; Eisenberg, R. *Organometallics* **1995**, *14*, 4525−4534.